JOURNAL OF MATERIALS SCIENCE 26 (1991) 5143–5148

EXAFS study of a hot-pressed α′-sialon ceramic containing erbium as the modifying cation

M. COLE, K. P. J. O'REILLY
Department of Chemistry, University of Keele, Staffordshire, ST5 5BG, UK
M. REDINGTON, S. HAMPSHIRE
Materials Research Centre, University of Limerick, Eire

The general composition for an α′-sialon is $M_x(Si, Al)_{12}(O, N)_{16}$, (the value of x lies between 0 and 2), where M is a modifying cation such as Li^+, Ca^{2+}, Y^{3+} or a number of the lanthanide cations (Ln^{3+}). This paper reports extended X-ray absorption fine structure (EXAFS) spectroscopy measurements of a hot-pressed erbium containing α′-sialon, using the synchrotron radiation source at Daresbury, UK. This technique provides short-range structural information within this engineering ceramic. The results suggest that the erbium modifying cation shows a preference for being located in one particular site within the ceramic network.

1. Introduction

α′-sialon ceramics have received considerable interest over the last 25 years because of their ease of preparation, thermal and chemical stability, low coefficient of thermal expansion and electrical conductivity. These give rise to potentially good engineering ceramics [1–7]. α′-sialons have the general composition of $M_x(Si, Al)_{12}(O, N)_{16}$, where $x \leqslant 2$ and M is a modifying cation such as Li^+, Ca^{2+}, Y^{3+} and most of the lanthanide (Ln^{3+}) ions [5, 7]. The structure of α′-sialons is derived from α-silicon nitride, which has a trigonal space group P31c [8], by partial replacement of Si by Al and N by O. The modifying cation maintains electrical neutrality by being "stuffed" into the structure. Crystallographic studies [9, 10] suggest that these modifying cations do occupy large closed interstices in the (Si, Al)–(N, O) network positioned at (0.333, 0.667, z) and (0.667, 0.333, 0.500 + z) [1, 4, 7, 9, 10]. These studies have provided an overall structure or long-range order description of the structure of these materials.

This work describes a preliminary study of the Er α′-sialon engineering ceramic material, $Er_{0.55}Si_{8.35}Al_{3.65}O_{0.8}N_{15.2}$, where the technique of extended X-ray absorption fine structure (EXAFS) spectroscopy has been used to investigate the local environment surrounding the Er^{3+} stabilizing cation. The technique of EXAFS exploits a rather subtle aspect of X-ray absorption. When X-rays pass through a material, it absorbs some of the radiation. It is found that the degree of absorption varies smoothly as the energy of the targeted X-rays is increased. However, at certain well defined energies, sharp increases in absorption are observed, these features being known as an "absorption edge". These absorption edges occur as a consequence of the X-rays having just the right amount of energy to kick out a core-energy-level electron from a particular atom within the sample. If the absorption of the X-rays causes photoelectrons to be ejected from the 1s energy level, then the absorption edge is known as the K-absorption edge. The corresponding absorption edges, as a consquence of the 2s and 2p electron excitations are known as the L-absorption edges. The L_I edge refers to the excitation of 2s electrons and the L_{II} and L_{III} edges refer to the 2p excitations.

EXAFS spectroscopy is manifested by the oscillations observed on the high-energy side of an X-ray absorption edge. These oscillations arise as a result of the interference effects between the outgoing photoelectron wave (invoked by means of core electron excitation by the X-ray beam) and the backscattered wave (caused by the reflection of the incident photoelectron wave by neighbouring atoms). The intensity and frequency of the EXAFS can be interpreted in terms of the number, nature and distance of the backscattering atoms adjacent to the absorbing atom [11]. The EXAFS technique clearly offers a very powerful tool to probe the local structure surrounding a particular type of atom or ion: it is "atom-specific". In addition, the EXAFS technique does not require the sample to be crystalline as in conventional X-ray diffraction techniques; the sample could be amorphous or even a liquid. There is the probability that the Er α′-sialon sample under investigation has a glassy secondary phase present which contains some erbium. Therefore, this could also contribute to the erbium EXAFS signal. However, the proportion of this secondary phase was small, < 5%, and was deemed to contribute a negligible EXAFS contribution.

0022–2461/91 $03.00 + .12

The mathematical representtion of the oscillatory EXAFS function $\chi(k)$ for a K-edge absorption, assuming that only single scattering of the photoelectron occurs and that the spherical photoelectron wave is approximated by a plane wave, can be described as in the following equation:

$$\chi(k) = \sum_j \frac{-N_j}{kR_j^2} |f_j(\pi)| \exp(-2\sigma_j^2 k^2) \times \exp(-2R_j/\lambda) \sin(2kR_j + 2\delta_1' + \psi_j \quad (1)$$

when atomic units are used. Here k is the momentum of the photoelectron ($k^2 = 2e$), N_j is the number of scattering atoms at a distance R_j, each with a back-scattering factor $|f_j(\pi)|$, and λ is the elastic mean free path of the photoelectron. The Debye–Waller term, $\exp(-2\sigma_j^2 k^2)$, is a measure of the thermal and static displacements within each shell, where σ_j^2 is the mean square variation in interatomic distance between the emitting and scattering atoms. δ_1' and ψ_j take into account the phase shifts experienced by the photoelectron wave on passing through the potentials of the absorbing atom and the jth shell atoms.

The strategy adopted in analysing EXAFS spectra of unknown structures is to reproduce the experimental data by a proposed model. With unknown structures, the values of $|f_j(\pi)|$, δ_1' and ψ_j are unknown and reliable values are required to give precise atomic positions. Normally, this is achieved by curve-fitting an EXAFS spectrum of a model compound of which the structure is known, and where the chemical environment surrounding the species under scrutiny is similar to that of the unknown material.

As already mentioned, the main aim of this study is to utilize the EXAFS technique in an attempt to gain an insight into the local structural features surrounding the stabilizing cation, Er^{3+}. The model compound used in this work was Er_2O_3, which although it is somewhat different to the ceramic material under investigation, did allow reasonable values for the phase-shift parameters to be obtained. Using these values, the only unknown parameters remaining in Equation 1 are N_j, R_j and σ_j^2, which could then be refined by least squares iteration using the new Daresbury EXAFS curve fitting program EXCURV90 [12]

2. Experimental procedure

The starting composition of $Er_{0.55}Si_{8.35}Al_{3.65}O_{0.8}N_{15.2}$ was prepared from a mixture of Er_2O_3 (Rare Earth Products Ltd, UK), Si_3N_4 (M. C. Stark, Berlin, West Germany) and AlN (M. C. Stark). These were wet-mixed in isopropanol for 30 min, followed by dry-mixing for 15 min to overcome the sedimentary effects caused by evaporating off the alcohol. The powder mixture was then first preformed into flat cylinder, with dimensions of 17.5 mm (diameter) and 4 mm (height), before being embedded in boron nitride under a pressure of 10 MPa for 30 min at 1750 °C in a graphite die. The sintered compact was then pulverized and submitted for X-ray powder diffraction analysis for phase identification. The sample (together with the Er_2O_3 model compound) were then ready for the EXAFS analysis.

The EXAFS measurements were performed at the SERC synchrotron radiation source (SRS) at Daresbury, where the Er (L_{III}) edge of each material was recorded. The datasets were collected using EXAFS station 7.1, where the measurements were taken under typical beam conditions of 2 GeV and 200 mA. The standard transmission mode EXAFS set-up was adopted, where the intensity of the X-ray beam is measured before and after the sample. All data were collected under conditions of ambient temperature and pressure.

3. Results

The EXAFS data fitting was achieved using the EXCURV90 program which uses a curved wave approximation, and which also calculates approximate phase-shifts for a specified central/neighbouring atom interaction. The bond distances and Debye–Waller factors together with a correction term ΔE_0 (which accounts for any inaccuracies in defining the position of the absorption edge of interest), were refined by a least squares iteration process.

All the data analysis involved a k-cubed weighting to enhance the features at high k where single scattering is most accurate. Inelastic scattering of the photoelectron was accounted for by an imaginary potential, V_{im}, which is related to the mean free path of the photoelectron, λ, by the following equation:

$$\lambda = \frac{-k \times (h/2\pi)^2}{2mV_{im}} \quad (2)$$

where h represents Planck's constant and m the mass of an electron. The amplitude reduction of the EXAFS oscillations caused by multiple excitations at the central atom/ion was also accounted for by using a reduction factor A_{red}. These two parameters, V_{im} and A_{red} were assigned values of -4.0 eV and 0.80, respectively, througout all the data deconvolution.

The theoretical parameters obtained by data fitting the model compound, Er_2O_3, are presented in Table I. For comparison, the established crystal structure data is also shown [13] (see Table II). It is observed that an excellent agreement between the two sets of values was obtained, thus indicating that the phase-shift parameters used were satisfactory. In this work, both analysed datasets (model compound and Er α′-sialon) had been Fourier-filtered so as to remove unwanted shell contributions.

TABLE I The EXAFS parameters obtained by fitting the model compound Er_2O_3

Shell	Atom type	Coordination no.	Distance (nm)	D–W Factor (nm^2)
1	O	6.0	0.2265	0.00019
2	Er	6.0	0.3489	0.00013
3	Er	6.0	0.3970	0.00018
4	Er	6.0	0.5246	0.00023
5	Er	12.0	0.6321	0.00036
6	Er	12.0	0.6582	0.00020

TABLE II The crystal structure data for the model compound Er_2O_3

Shell	Atom type	Coordination no.	Distance (nm)
1	O	6.0	0.2263
2	Er	6.0	0.3496
3	Er	6.0	0.3980
4	Er	6.0	0.5275
5	Er	12.0	0.6328
6	Er	12.0	0.6608

In Fig. 1, the "raw" Er L_{III} edge EXAFS data of the $Er_{0.55}Si_{8.35}Al_{3.65}O_{0.8}N_{15.2}$ is shown. The background absorption features which are superimposed on the EXAFS oscillations were removed by fitting polynomial functions to both the pre-edge and post-edge regions of the experimental spectrum. Fig. 2 shows the experimental (solid line) EXAFS oscillations after background subtraction had been carried out. The figure also shows the 'best-fit' theoretical curve (represented by the dashed line) to the experimental curve. Fig. 3 illustrates the accompanying experimental (solid line) and theoretical (dashed line) radial distribution Fourier transforms. It is quite obvious that a good agreement between the experimental data and the proposed theoretical model has arisen.

The least-squares refinement started from a set of parameter values derived from the Y α′-sialon work of Izumi *et al.* [10]. However, not all the shells were fitted in the EXAFS data analysis, because they were deemed to give a negligible EXAFS contribution. The shells that were omitted were (N, O) shells with a coordination number of three or less at a distance greater than 0.32 nm, as the effect of the electron backscattering ability of these shells is relatively weak. Data fitting to the experimental data finally gave the fits in Figs 2 and 3 with the refined local parameters as presented in Table III. The energy window used was $E_{min} = 34.21$ eV, and $E_{max} = 636.59$ eV. The Er α′-sialon dataset was Fourier-filtered at $R_{min} = 0.161$ nm, and $R_{max} = 0.574$ nm.

TABLE III The refined EXAFS parameters obtained by fitting the Er α′-sialon ceramic

Shell	Atom type	Coordination no.	Distance (nm)	D–W factor (nm^2)
1	O	2.0	0.2257	0.00010
2	N	5.0	0.2480	0.00031
3	Si	2.0	0.2914	0.00019
4	N	3.0	0.3174	0.00008
5	Si	6.0	0.3177	0.00019
6	Si	3.0	0.3502	0.00022
7	Si	3.0	0.3755	0.00024
8	Al	1.0	0.4094	0.00017
9	Si	3.0	0.4596	0.00048
10	N	6.0	0.4684	0.00020
11	Si	3.0	0.5221	0.00017
12	Si	3.0	0.5381	0.00006
13	Si	6.0	0.5534	0.00018
14	Er	1.0	0.5687	0.00015

$\Delta E_0 = 12.03$ eV; VPI = −4.00 eV; AFAC = 0.80; $E_{min} = 34.21$ eV; $E_{max} = 636.59$ eV; k^3 Fit index = 0.0507; R-factor = 10.678%

In Table III, the results are given in increasing radial distance relative to the central or targeted Er^{3+} cation. For comparison, Table IV shows a similar set of values that have been derived from the Izumi structure refinement of the Y α′-sialon. Tables III and IV have been laid out for easy comparison of the two systems.

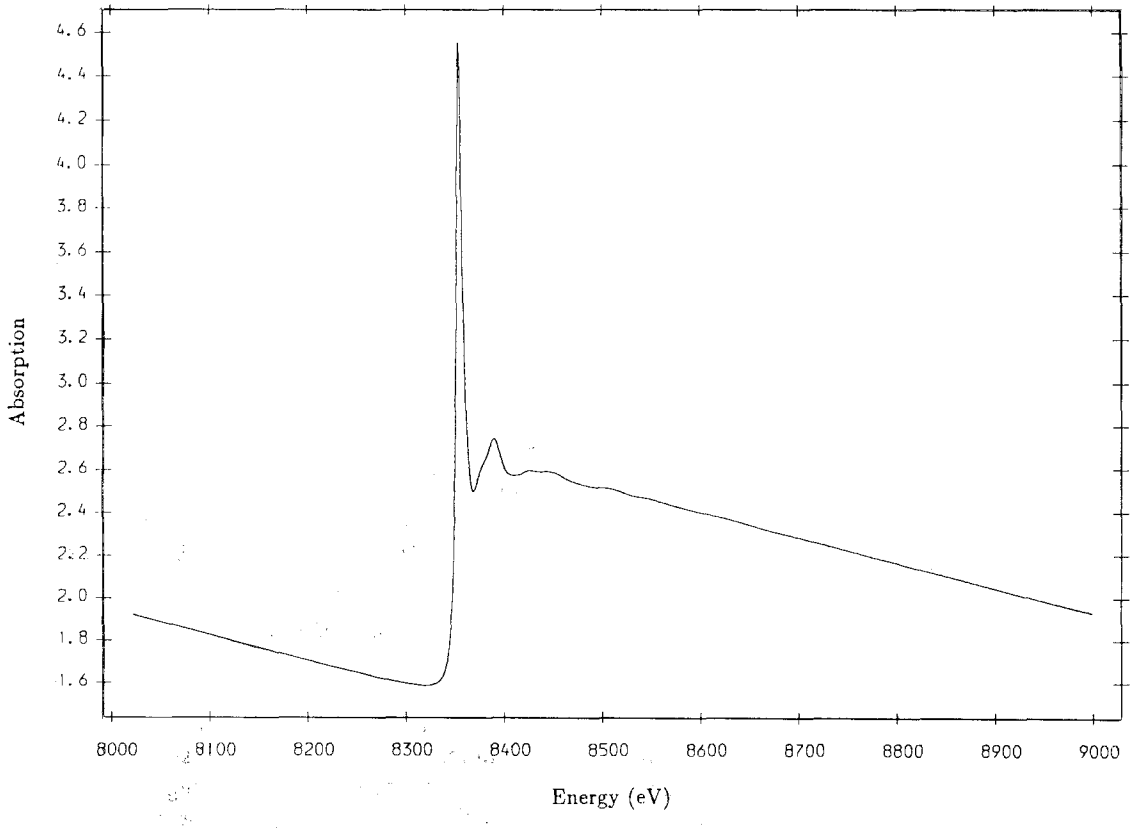

Figure 1 Absorption spectrum of the Er α′-sialon—(Er L_{III} edge)

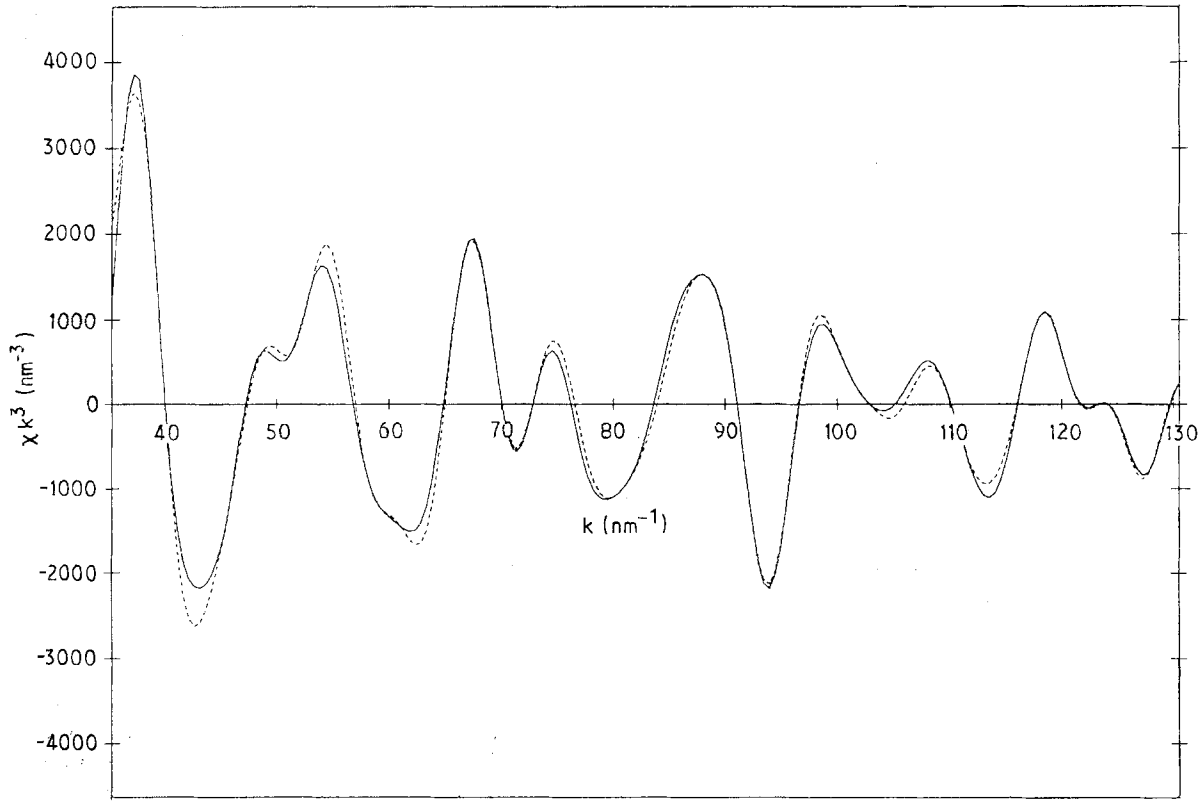

Figure 2 Experimental (——) and theoretical (– – –) EXAFS oscillations of the Er α′-sialon

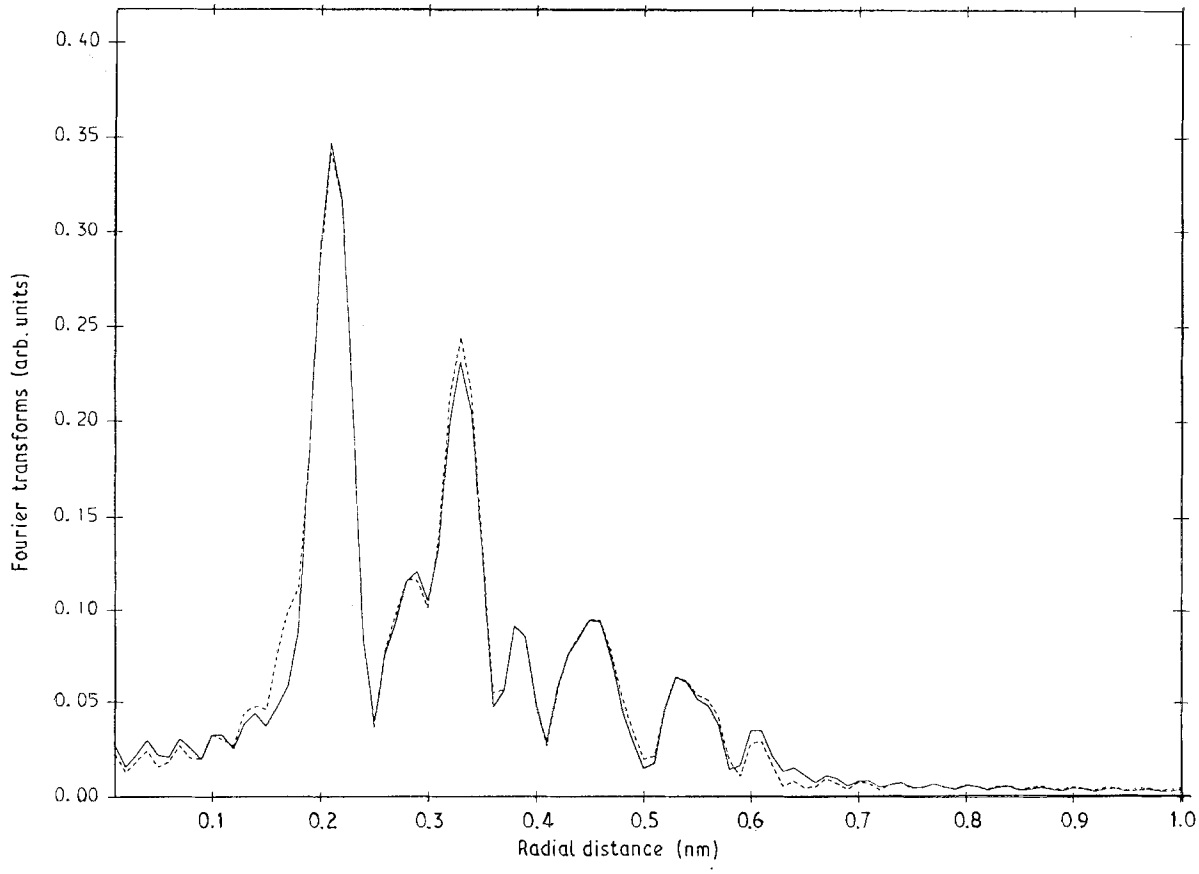

Figure 3 The corresponding experimental (——) and theoretical (– – –) Fourier transforms of the Er α′-sialon

The EXAFS refinement of the Er α′-sialon shows a radial function at ~ 0.24 nm, indicating one broad, large peak. This broad peak refines into two shells of which one contains oxygen and the other nitrogen, as shown in Table III. These two shells of two oxygens at a bond distance of 0.2257 nm, and five nitrogens at distance of 0.2480 nm, are associated with the Er^{3+} actions in the interstices having seven-fold coordination. One slight difference between the EXAFS refinement and the Izumi Rietveld refinement, is that

TABLE IV The crystal structural data of the Y α′-sialon ceramic [10]

Shell	Atom type	Number of sites*	Distance (nm)
1	$(N, O)_2$	1.0	0.2346
2†	$(N, O)_3$, $(N, O)_4$	6.0	0.2646
3	$(Si, Al)_1$	3.0	0.2832
4	$(N)_3$	3.0	0.3128
5†	$(Si)_1$, $(Si, Al)_2$	6.0	0.3166
‡	$(N, O)_2$	1.0	0.3362
6	$(Si)_1$	3.0	0.3477
‡	$(N)_4$	3.0	0.3872
7	$(Si)_2$	3.0	0.3905
‡	$(N)_4$	3.0	0.3905
8	¶	–	–
9	$(Si)_2$	3.0	0.4546
‡	$(N)_2$	3.0	0.4546
10	$(N, O)_1$	6.0	0.4727
‡	$(N)_1$	3.0	0.4754
‡	$(N, O)_3$	3.0	0.4825
‡	$(N, O)_4$	6.0	0.5116
11	$(Si, Al)_2$	3.0	0.5176
‡	$(N)_3$	3.0	0.5300
§	$(Y)_1$	6.0	0.5346
12	$(Si, Al)_1$	3.0	0.5400
13†	$(Si, Al)_1$, $(Si, Al)_2$	6.0	0.5537
14	$(Y)_1$	2.0	0.5708

* The phrase 'number of sites' is used for the (Si, Al) and (N, O) sites to indicate coordination numbers. For the Y sites, the phrase is used to denote number of possible sites available for occupation (not coordination number).
† Average of two close shells.
‡ EXAFS contribution negligible.
§ No corresponding shell found in the EXAFS analysis.
¶ No corresponding shell to that in the Er α′-sialon.

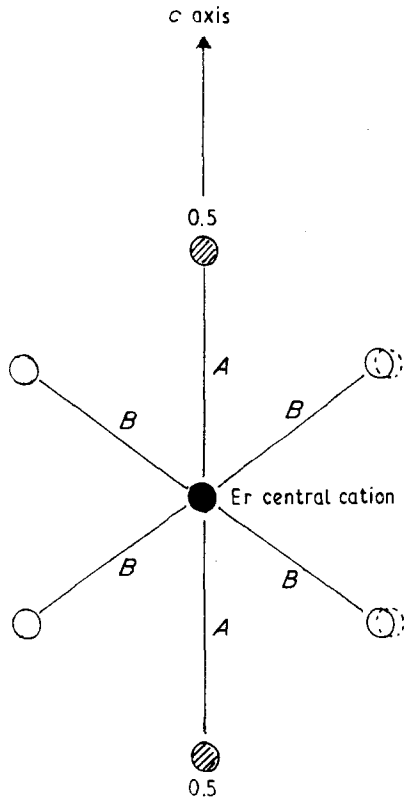

Figure 4 An illustration of the spatial arrangement of the interstices within α′-sialons. $A = 0.5687$ nm; $B = 0.5346$ nm.

instead of the 2 : 5 ratio of the two shells, the Japanese group suggested this seven-fold nearest neighbour coordination shell consisted of a 1 : 6 ratio.

In addition, the EXAFS refinement shows that when the bond distances of the modifying cation to the members of this seven-fold coordination shell are compared with those of the Yα′-sialon, they are significantly shorter: the presence of the Er^{3+} cation pulls both the oxygen and nitrogen nearest neighbour species towards itself. For example, in the case where the modifying cation is Y^{3+}, the bond distances of the first two shells are 0.2346 and 0.2646 nm, whereas the EXAFS refinement indicated bond distances of 0.2257 and 0.2480 nm. Since the two different modifying cations are almost identical in size (Er^{3+}, 0.0881 nm; Y^{3+} 0.0893 nm) this "pulling-in" effect could be a consequence of the Er^{3+} cations being positioned or arranged differently to the Y^{3+} cations. It is also observed that the opposite trend occurs when shell 3 of each system is considered, where the presence of the Er^{3+} cations appear to repel or "push-out" the Si species relative to that of the Y system. In the case of the Y α′-sialon the bond distance was reported to be 0.2832 nm, whereas the EXAFS refinement indicated a bond distance of 0.2914 nm.

As already suggested, these differences between the two structures could be a result of the modifying cations having a different positional arrangement. In the case of the Y α′-sialon structure, the Y^{3+} "central" cation located in its interstice, has eight possible neighbouring interstices which could accommodate other modifying cations. Izumi *et al.* [9, 10] indicated there were six potential Y–Y interactions possible at a bond distance of 0.5346 nm, and two others (in the *c*-axis direction, one above and one below) at a distance of 0.5708 nm, (see Fig. 4). However, it was stated that these eight sites were only partially occupied, but with no indication as to which ones were occupied. The composition used by the Japanese group was such that there was half a Y^{3+} species on average per unit cell, with each unit cell having two interstices at a distance of 0.5346 nm. Therefore, all the eight sites situated around the 'central' Y^{3+} cation would not be filled. However, this work did not indicate if any preferred orientations would arise, or whether the adjacent cation would prefer to reside at a bond distance of 0.5346 nm, or at the site situated at a bond distance of 0.5708 nm.

The EXAFS refinement of the Er α′-sialon indicates that there is only one Er–Er interaction which occurs at a bond distance of 0.5687 nm. No electron density corresponding to that which could be attributed to the 'heavy' backscattering of neighbouring Er^{3+} cations could be found at 0.5346 nm despite repeated attempts to "lure" these species into this shell. This tends to suggest that the Er^{3+} cations display a preferred orientation along the *c*-axis as illustrated in Fig. 4. The EXAFS analysis suggests that on average the coordination number corresponding to this *c*-axis Er–Er interaction is ~ 1. Since the starting composition was one that on average would lead to $\sim Er_{0.5}$ per unit cell, this would then agree with the overall coordination number of 1 (two sites each with an effective coordination number of 0.5). This preferred siting

along the c-axis could cause a uniform radial attraction on the (N, O) species and may therefore cause the "pulled" effect of the (N, $O)_2$, (N, $O)_3$ and (N, $O)_4$ positions towards the cations.

The overall Al content corresponding to the starting composition should be $Al_{3.65}$ per unit cell. Only a fraction of this is indicated by the EXAFS study and this may be due to different Si/Al replacement sites occurring, making the Al distribution totally random. Thus the EXAFS technique would find it difficult to discern a predominant Al site. The fit started off with the Al being situated in the shell 3 site ($\sim$ 0.283 nm) which would make sense from simple electrostatic arguments. However, the refinement indicated that this was not a realistic position for the Al species because of the high Debye–Waller factor term associated with this siting. The EXAFS fit was improved remarkably when this Al position was pushed out to about 0.4 nm.

The overall oxygen content corresponding to the starting composition should be $O_{0.8}$ per unit cell. However the EXAFS fit has indicated an oxygen content much higher than this. One possible explanation for this could be due to the fact that the starting composition was more oxygen rich due to the surface silica on the silicon nitride not being taken into account.

In general, the remaining shells containing (Si, Al) or (N, O) of the Er system follow the same trends but not to the same degree. In both sets of values the bond distances remain similar with each other, with the exception of shell no. 7 where there is a discrepancy of about 0.015 nm. A possible reason for these 'further-out' shells having comparable values, whereas the three nearest neighbour shells show significant differences, could be that further away from the central cation, any electrostatic attractions and/or repulsions will be dampened.

4. Conclusions

This work has been concerned with the study of the local structural features surronding the Er^{3+} cationic species in the Er α'-sialon, $Er_{0.55}Si_{8.35}Al_{3.65}O_{0.8}N_{15.2}$, using EXAFS. The EXAFS data refinement has provided strong evidence that the Er^{3+} modifying cations adopt a preferred orientation arrangement along the c-axis. This study is the first to indicate that such a preferred siting occurs within α'-sialons. It is tentatively postulated that if the cation content is increased, all the c-axis positions will be filled up first. This work also confirms the seven-fold coordination of the modifying cation within the interstices, but indicates a N : O ratio of 5 : 2 rather than the 6 : 1 ratio as indicated by the Rietveld refinements of Izumi *et al.* Finally, it is suggested that the overall distortion of the (Si, Al) and (N, O) shells will vary with the choice of modifying cation used, together with the intersticial occupancy state which is dependent on the modifying cation content.

References

1. S. HAMPSHIRE, H. K. PARK, D. P. THOMPSON and K. H. JACK, *Nature* **274** (1978) 880.
2. G. GRAND, J. DEMIT, J. RUSTE and J. P. TORRE, *J. Mater. Sci.* **14** (1979) 1749.
3. M. MITOMO, H. TANAKA, K. MURAMATSU, N. II and Y. FUJII, *ibid.* **15** (1980), 2661.
4. H. K. PARK, D. P. THOMPSON and K. H. JACK, in "Science of Ceramics", Vol. 10, edited by H. Hausner (Deutsche Keramische Gesellschafr. Germany, 1980) p. 251.
5. M. MITOMO and Y. UEMURA, *J. Mater. Sci.* **16** (1981) 552.
6. Z-K. HUANG, P. GREIL and G. PETZOW, *J. Amer. Ceram. Soc.* **66** (1983) C-96.
7. K. H. JACK, in "Progress in Nitrogen Ceramics", edited by F. L. Riley (Martinus Nijhoff, The Hague, 1983) p. 45.
8. R. MARCHAND, Y. LAURENT and J. LANG, *Acta Crystallogr.* **B25** (1969) 2157.
9. F. IZUMI, M. MITOMO and J. SUZUKI, *J. Mater. Sci. Lett.* **1** (1982) 533.
10. F. IZUMI, M. MITOMO and Y. BANDO, *J. Mater. Sci.* **19** (1984) 3115.
11. J. STÖHR, in "Emission and Scattering Techniques", edited by P. Day (Reidel Dordrecht, The Netherlands, 1981), p. 213.
12. N. BINSTED, S. J. GURMAN and J. W. CAMPBELL, "SERC Daresbury Laboratory EXCURV90 program" (1990).
13. A. SAIKI, N. ISHIZAWA, N. MIZUTANI and M. KATO, *J. Ceram. Assoc. Jpn* **93** (1985) 649.

Received 14 May
and accepted 26 June 1990